

STRATIGRAPHY AND EVOLUTION OF DELTA CHANNEL DEPOSITS, JEZERO CRATER, MARS.

T. A. Goudge¹, D. Mohrig¹, B. T. Cardenas¹, C. M. Hughes¹, and C. I. Fassett², ¹Jackson School of Geosciences, The University of Texas at Austin, Austin, TX, ²NASA Marshall Space Flight Center, Huntsville, AL. (Contact: tgoudge@jsg.utexas.edu)

Introduction: The Jezero impact crater hosted an open-basin lake [1] that was active during the valley network forming era on early Mars [2]. This basin contains a well exposed delta deposit at the mouth of the western inlet valley (Fig. 1) [1,3-5]. The fluvial stratigraphy of this deposit provides a record of the channels that built the delta over time. Here we describe observations of the stratigraphy of the channel deposits of the Jezero western delta to help reconstruct its evolution.

Methods: We use orthorectified HiRISE images [6] and stereo-derived digital elevation models (DEMs) to map the channel deposit stratigraphy of the upper portion of the deposit (Fig. 1), which we interpret as the exhumed topset of the delta. We use HiRISE DEMs produced with the NASA Ames Stereo Pipeline [7-9] to extract quantitative characteristics of the geometries of the channel deposits.

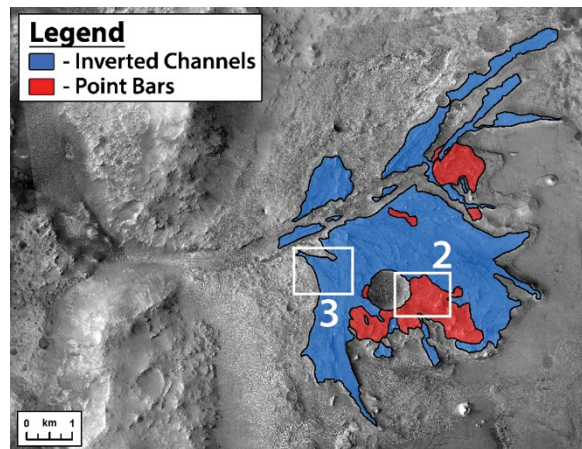


Fig. 1. Mapped Jezero western delta channel deposit stratigraphy. White boxes indicate locations of Figs. 2A and 3A. Mosaic of CTX [10] image D14_032794_1989 and HiRISE images PSP_003798_1985, ESP_037396_1985 and ESP_036618_1985.

Jezero Fluvial Stratigraphy: We map two classes of channel deposit stratigraphy of the Jezero western delta (Fig. 1): point bars and inverted channel-fills. We interpret these deposits as indicative of distinct types of fluvial channels associated with the growth of the delta.

Point Bar Deposits: The stratigraphically lower class is alternating dark- and light-toned curved strata (Fig. 2). We interpret these as eroded lateral accretion packages of point bar deposits built on the inner banks of channel bends [e.g., 11,12]. Point bar growth primarily occurs at flood stage, and each stratum in the point-bar deposits of the Jezero delta likely records a single flood event [11]. The large number of point bar strata

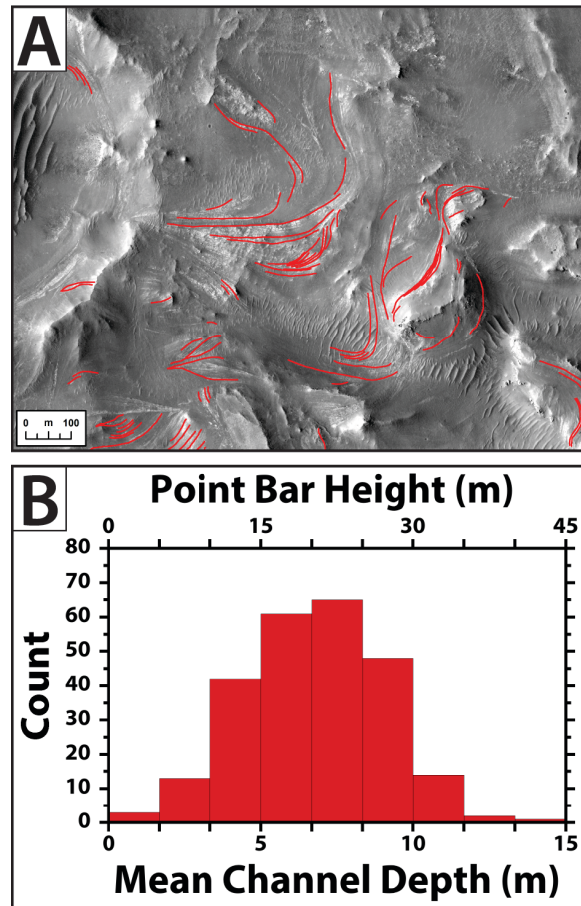


Fig. 2. (A) Example mapped point bar deposits (red traces). Portion of HiRISE image ESP_037396_1985. (B) Histogram of modeled point bar heights and corresponding mean channel depths.

that make up coherent accretional units (Fig. 2A) suggest that the climate under which the delta was built experienced regional flooding modulated at non-orbital timescales (e.g., yearly to decadal).

Channel lateral migration rates and point bar growth significantly decrease in the reaches of the river most proximal to the shoreline [13,14]. Therefore, the mapped point bar deposits record meandering channels supplying water and sediment to a Jezero paleolake shoreline still located at some distance from the site of deposition. This is consistent with outcrops of deltaic sediment identified farther towards the basin center [4].

To estimate the geometry of the formative meandering channels, we fit the mapped point bar strata with a downward opening paraboloid from which we estimated the model point bar height. Point bars record the bank-

full relief at a channel bend, which can be up to ~ 3 times larger than mean bank-full flow depth (assuming approximately constant channel width) [15]. Results from our modeled point bar surfaces suggest formative mean channel depths of ~ 5 –10 m (**Fig. 2B**).

Inverted Channel-Filling Deposits: Overlying the point bar deposits is a succession of stacked, approximately straight ridges (**Fig. 3**). We interpret these ridges as inverted channel-filling deposits [1,4], formed from the topographic inversion of sediment deposited within channels preserving little to no evidence for lateral mobility of bends.

Both the stacked nature of the channel bodies and the wide range in modeled transport directions indicate a highly dynamic system with frequent channel avulsions. Avulsions occur as a channel responds to super-elevation relative to the surrounding terrain by selecting a new, lower potential energy path [16], a process driven by channel bed aggradation [16,17]. The primary cause for channel bed aggradation here is interpreted to be water level rise and shoreline transgression, indicated by backstepping channel body elevations (**Fig. 3B**).

To estimate the geometry of the formative avulsive channels, we measure the thickness of individual channel bodies, which has been shown to provide a robust proxy for channel depth [16]. Results indicate formative channel depths of $< \sim 2$ m (**Fig. 3C**).

Jezero Delta Evolution: The stratigraphy and geometry of the Jezero western delta channel deposits record two styles of channelization and associated sedimentation: (1) fluvial facies of deeper meandering channels that formed some distance upstream from the paleolake shoreline (**Fig. 2**), and (2) coastal facies of shallower channels that formed proximal to the paleolake shoreline (**Fig. 3**).

We interpret the stratigraphic signature of coastal facies overlying fluvial facies as indicative of autoretreat [18,19]. Autoretreat occurs under conditions of rising water level and approximately constant sediment supply, as the input sediment load becomes insufficient to fill the increasing accommodation space [18,19].

We conclude that the Jezero western delta primarily records the filling of the basin to an overtopping level [1]. Importantly, we observe no major erosional unconformities or alternation of channel deposit class up-section. This indicates a lack of major lake level drops during filling of the basin, suggesting a climate during delta growth with persistent surface runoff.

References: [1] Fassett, C., J. Head (2005), *GRL*, **32**:L14201. [2] Fassett, C., J. Head (2008), *Icarus*, **198**:37–56. [3] Ehmann, B., et al. (2008), *Nat. Geosci.*, **1**:355–358. [4] Schon, S., et al. (2012), *PSS*, **67**:28–45. [5] Goudge, T., et al. (2017), *EPSL*, **458**:357–365. [6] McEwen, A., et al. (2007), *JGR*, **112**:E05S02. [7] Broxton, M., L. Edwards (2008), *LPSC* 39, #2419. [8] Moratto, Z., et al. (2010), *LPSC* 41, #2364. [9] Shean et al. (2016), *ISPRS J. Phot. Rem. Sens.*, **116**:101–117.

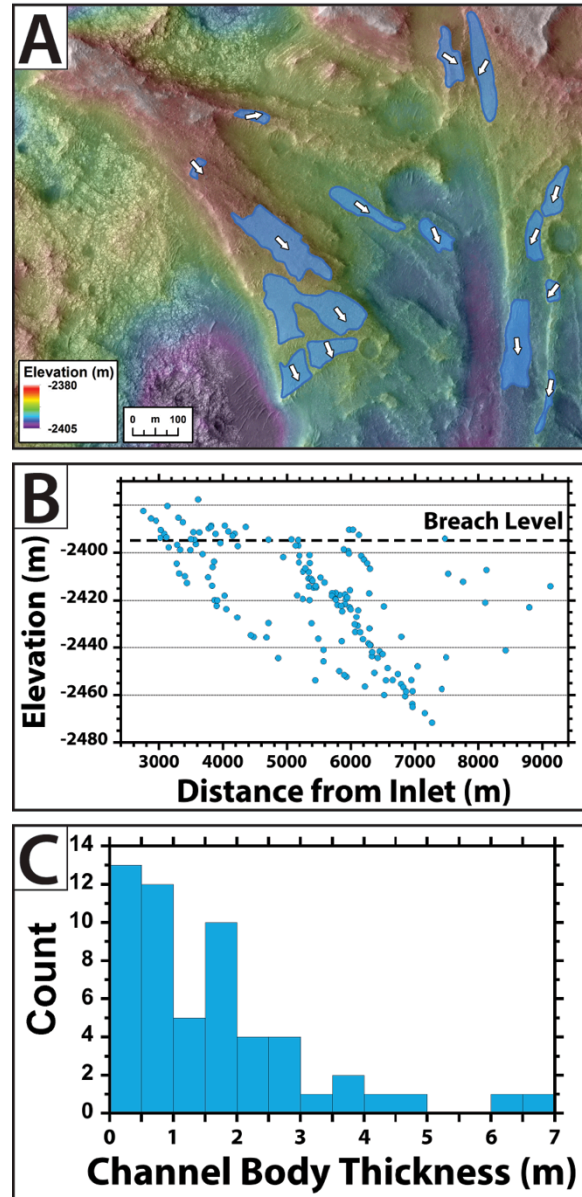


Fig. 3. (A) Example mapped inverted channel-filling deposits (blue outlines). White arrows show modeled transport direction. HiRISE-derived DEM from images ESP_037396_1985 and ESP_042315_1985 overlain on HiRISE image ESP_037396_1985. (B) Mean elevation vs. distance from the inlet for modeled channel bodies. (C) Histogram of measured channel body thicknesses.

[10] Malin et al. (2007), *JGR*, **112**:E05S04. [11] Allen, J. (1965), *Sedimentology*, **5**:89–191. [12] Parker, G., et al. (2011), *Earth Surf. Process. Landforms*, **36**:70–86. [13] Hudson, P., R. Kesel (2000), *Geology*, **28**:531–534. [14] Nitttrouer, J., et al. (2012), *GSA Bull.*, **124**:400–414. [15] Bridge, J., S. Mackey (1993), in *IAS Spec. Pub. 15*, pp. 213–236. [16] Morig, D., et al. (2000), *GSAB*, **112**:1787–1803. [17] Bryant, M., et al. (1995), *Geology*, **23**:365–368. [18] Muto, T., R. Steel (1992), *Geology*, **20**:967–970. [19] Muto, T. (2001), *J. Sed. Res.*, **71**:246–254.